Journal of Inorganic Biochemistry 196 (2019) 110685

Contents lists available at ScienceDirect

Journal of Inorganic Biochemistry

journal homepage: www.elsevier.com/locate/jinorgbio

Inactivation of NikR from *Helicobacter pylori* by a bismuth drug

Yu Guo[a], Chujun Guan[a], Heiyu Wan[a], Zhengrui Zhang[a], Hongyan Li[b], Hongzhe Sun[b,*], Wei Xia[a,*]

[a] MOE Key Laboratory of Bioinorganic and Synthetic Chemistry, School of Chemistry, Sun Yat-sen University, Guangzhou, China, 510275
[b] Department of Chemistry, The University of Hong Kong, Pokfulam Road, Hong Kong, China

ARTICLE INFO

Keywords:
Helicobacter pylori
Bismuth drug
DNA regulator
Metal-binding

ABSTRACT

The NikR protein is an essential DNA regulator of *Helicobacter pylori*, a human pathogen, which infects almost half of the world's population. Herein, we comprehensively characterized the interaction of a bismuth drug with *Helicobacter pylori* NikR. We show that Bi(III) can occupy the high-affinity Ni(II) site of NikR. The highly-conserved residue Cys107 at this site is critical for Bi(III) binding. Importantly, such a binding disassembles physiologically functional NikR tetramer into inactive dimer, leading to abrogation of the DNA-binding capability of NikR. Bi(III)-binding also significantly disturbs regulatory function of *Helicobacter pylori* NikR *in vivo*. Therefore, NikR might serve as a potential intracellular target of a bismuth drug.

1. Introduction

Helicobacter pylori (*H. pylori*) is a worldwide spread pathogen that can colonize in human gastric mucosa. *H. pylori* infection causes a series of gastrointestinal diseases, including chronic gastritis, peptic ulcer and even gastric cancer [1]. Two obligate nickel-containing enzymes, urease and hydrogenase, play a crucial role in the survival of this bacterium under highly-acidic environment in human stomach. Urease hydrolyzes urea into ammonia and bicarbonate to neutralize the gastric acids and raise the local pH [2,3]. While hydrogenase allows *H. pylori* to utilize the hydrogen gas produced by other host flora as an energy source [4]. Although transition metal nickel is an essential nutrient for *H. pylori*, the intracellular nickel distribution is tightly controlled due to its intrinsic toxicity. In *H. pylori*, nickel homeostasis is primarily regulated by a nickel-responsive transcription factor NikR [5–8].

H. pylori NikR (*Hp*NikR) is a pleiotropic regulator and controls the expression of a large set of genes involved not only in nickel homeostasis but also in iron metabolism as well as acid stress response [3,6,9]. Therefore, *Hp*NikR is considered as a global regulator and exerts a critical role in *H. pylori* colonization, adaption and survival in human gastric mucosa. *Hp*NikR is a tetrameric protein and each monomer is composed of two domains, an N-terminal DNA-binding domain (DBD) and a C-terminal metal-binding domain (MBD) [7,8,10,11]. The activation of *Hp*NikR depends on the incorporation of nickel ions to a conserved high-affinity nickel binding site (HA site) at MBD (Fig. 1), which consists of a cysteine and two histidines (Cys107, His99 and His101) from one subunit and an additional histidine (His88′) from the adjacent subunit [11–16]. Ni(II) coordination to the HA site increases the orientation mobility of DBD with respect to the MBD, which promotes tight DNA binding of *Hp*NikR [8,12,17–20]. Importantly, the *Hp*NikR HA site is nickel specific, since other divalent metal ions cannot activate *Hp*NikR for DNA binding [13,16].

Bismuth compounds, such as bismuth subsalicylate (BSS) and colloidal bismuth subcitrate (CBS) [21,22] have been widely used to treat *H. pylori* infection [23–25]. Although significant progress has been made to understand the inhibitory mechanism of bismuth compounds, the bismuth-binding targets are not fully unveiled [26,27]. Due to the thiophilic nature of Bi(III), its biological targets are predominantly proteins rich in thiol-containing cysteine residues [28,29]. Recently, we have identified the ferric uptake regulator (Fur) of *H. pylori* as one of the important targets of bismuth drugs. Bi(III) binding causes Fur dysfunction, which leads to disruption of iron metabolism in *H. pylori* [30]. The HA site of *Hp*NikR is composed of one cysteine and three histidine residues. Given the highly thiophilic feature of bismuth and significantly bigger ion radius compared with nickel, it is reasonable to speculate that Bi(III) could probably occupy the HA site and interfere with the physiological function of *Hp*NikR. Herein, we have comprehensively characterized the interaction between *Hp*NikR and Bi(III). The data demonstrate that *Hp*NikR is a potential Bi(III)-binding target *in vitro* as well as *in vivo*. Importantly, Bi(III)-binding ruptures functionally tetrameric *Hp*NikR and disturbs transcriptional level of genes regulated by *Hp*NikR.

2. Materials and methods

All chemicals were purchased from Sigma-Aldrich unless otherwise stated. The *Hp*NikR polyclonal antibodies were prepared by

* Corresponding authors.
E-mail addresses: hsun@hku.hk (H. Sun), xiawei5@mail.sysu.edu.cn (W. Xia).

https://doi.org/10.1016/j.jinorgbio.2019.03.025
Received 21 January 2019; Received in revised form 21 March 2019; Accepted 28 March 2019
Available online 08 April 2019
0162-0134/

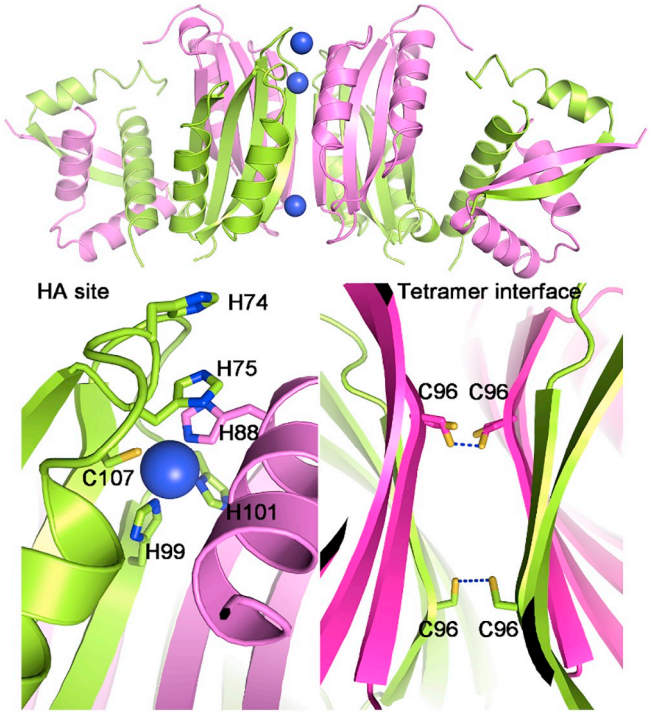

Fig. 1. Crystal structure of Ni(II) bound *Hp*NikR tetramer (protein data bank code 2CAD). The high-affinity (HA) and the tetramerization interface of *Hp*NikR are shown. The potential bismuth binding residues and cysteine residues at the tetramer interface are shown in sticks.

immunizing rabbits with purified *Hp*NikR protein (Huabio, China). The antibodies were purified from antisera by Protein A sefinose (Sangon, China). *Escherichia coli* (*E. coli*) BL21(DE3) and XL1-Blue strains were cultured in Luria-Bertani (LB) medium with required antibiotics. *Helicobacter pylori* (*H. pylori*) 26695 strain was cultured in Brucella Broth (BB) medium supplemented with 0.2% *β*-cyclodextrin. Primers are listed in Table S1.

2.1. Expression and purification Apo-HpNikR

nikR gene was amplified by polymerase chain reaction (PCR) using *H. pylori* strain 26695 genomic DNA as a template with the primers listed in Table S1. The amplified *nikR* gene (hp1338) was digested with BamHI and *Hin*dIII restriction enzymes and ligated into pET47b plasmid, which has been digested with the same restriction enzymes. The generated NikR-pET47b plasmid was transformed into *E. coli* BL21(DE3) for protein expression. Overnight culture of BL21(DE3) strain that contains the NikR-pET47b plasmid was diluted by 1:100 to fresh LB medium supplemented with 50 μg/mL Kanamycin and grown for 3 h aerobically at 37 °C until OD_{600} reached around 0.6. Protein expression was induced by addition of isopropyl-β-d-thiogalactoside (IPTG) to a final concentration of 0.2 mM and bacteria were further cultured at 25 °C overnight. The bacteria were harvested by centrifugation and the cell pellets were resuspended in 40 mL of buffer 1 [20 mM 4-(2-hydroxyethyl)-1-piperazineethanesulfonic acid (HEPES), 300 mM NaCl, 1 mM phenylmethanesulfonyl fluoride (PMSF), pH 7.5] and lysed by sonication at 4 °C. The supernatant was subsequently dialyzed against buffer 2 [50 mM NaCl, 20 mM Tris-HCl, 1 mM dithiothreitol (DTT), 100 mM ethylene diamine tetra acetic acid (EDTA), pH 8.0] at 4 °C overnight. The supernatant was then applied onto a 5 mL HiTrap Q HP column (GE Healthcare). Elution was performed with a linear gradient from 0 to 500 mM NaCl. The eluted fractions were treated with 100 mM EDTA at 4 °C overnight to remove bound metal ions and further purified by Mono Q and Hiload 16/60 Superdex 200 16/60 column pre-equilibrated with buffer 3 [20 mM HEPES, 300 mM NaCl, 0.5 mM tris(2-carboxyethyl)phosphine (TCEP), pH 7.5]. Protein purity was higher than 95% as confirmed by sodium dodecyl sulfate polyacrylamide gel electrophoresis (SDS-PAGE) (Fig. S1). Purified apoform *Hp*NikR was concentrated to 10 mg/mL and stored at −80 °C. Plasmids for the variants were generated *via* Quick-Change mutagenesis using Wild-type NikR-pET47b as DNA template. Primers used for mutagenesis are listed in Table S1. The expression and purification of *Hp*NikR variants were similar to those of wild-type *Hp*NikR.

2.2. UV–vis spectroscopy

UV–vis spectroscopy was employed to monitor binding of Bi(III) to *Hp*NikR. Aliquots of 2 mM CBS were added into 40 μM *Hp*NikR in buffer 3 (20 mM HEPES, 300 mM NaCl, 500 μM TCEP, pH 7.5). UV–vis spectra were recorded on a UV-2600 spectrophotometer (SHIMADZU) at ambient temperature after equilibrium for 15 min. All experiments were performed in triplicate.

2.3. Inductively coupled plasma mass spectrometry

The metal contents of protein were determined by inductively coupled plasma mass spectrometry (ICP-MS). All ICP-MS experiments were conducted on a Thermo Scientific iCAP Q ICP-MS spectrometer. 4 molar equivalents of Bi(III) were added into 15 μM *Hp*NikR or variants. After incubation for 60 min at room temperature, excess amounts of Bi(III) were removed by HiTrap desalting column (GE healthcare). The eluted protein concentrations were measured by bicinchoninic acid (BCA) assay. And the bound Bi(III) contents were determined by ICP-MS. Each sample was quantified in triplicate and the average value was used.

2.4. Circular dichroism spectroscopy

Circular dichroism (CD) spectra of *Hp*NikR and variants were collected on a Jasco-810 spectrophotometer. 8 μM protein was pre-incubated with different molar equivalents Bi(III) as indicated in buffer 4 (20 mM HEPES, 50 mM NaCl, 0.5 mM TCEP, pH 7.5) at ambient temperature for 30 min. The CD spectra were recorded from 200 to 250 nm at a scan rate of 50 nm/min in a 0.1 cm quartz cuvette at ambient temperature. Three scans were averaged for each spectrum and the reference spectrum of the buffer was subtracted.

2.5. Size-exclusion chromatography

The oligomerization states of *Hp*NikR and variants were analyzed by size-exclusion chromatography (SEC). SEC was performed on a Tricorn Superdex 200 10/300 GL increase analytical column (GE Healthcare) at 4 °C. The column was pre-equilibrated with buffer 3 (20 mM HEPES, 300 mM NaCl, 0.5 mM TCEP, pH 7.5). 50 μM *Hp*NikR or variants were incubated with different molar equivalents of $Bi(NO)_3$ at room temperature for 30 min. The samples were subsequently loaded into SEC column at 0.5 mL/min. The column was calibrated with GE low molecular weight calibration kit under the same buffer condition.

2.6. Electrophoretic mobility shift assays (EMSA)

DNA-binding capability of *Hp*NikR and variant were examined by EMSA. The promoter DNA of *ureA* gene for EMSA was generated by PCR using *H. pylori* genomic DNA as a template with primer pairs listed in Table S1. The reaction was performed in binding buffer (20 mM Borate Bis-Tris, 800 μM $NiSO_4$, 50 mM KCl, 3 mM $MgCl_2$, 0.1% Triton X-100 and 0.5% glycerol, pH 7.4) with a final volume of 10 μL. For Ni(II)-dependent DNA binding, the reaction mixture contained 80 nM DNA and different concentrations of *Hp*NikR (0, 20, 50, 80, 100, 200 and 400 nM). In Bi(III) perturbation assay, *Hp*NikR or *Hp*NikR$^{H74A/H75A}$ were first incubated with gradient amounts of Bi(III) (0, 0.125, 0.25,

1.25, 2.5, 10, 20 molar equivalents). DNA and protein was subsequently mixed in reaction buffer to a final concentration of 80 nM and 400 nM, respectively. Finally, 10 μL of the reaction samples were applied into a 6% (w/v) native polyacrylamide Borate bis-Tris (TB) gel and electrophoresed in 0.5 × TB (v/v) buffer for 50 min at 125 V. Gel was stained in a 10,000-fold diluted Gene-Finder nucleic acid staining solution (Xiamen Zhishan Ltd, China) for 5 min. The DNA bands were visualized with blue light trans-illuminator (Syngene).

2.7. Cellular thermal shift assay (CETSA)

CETSA melting curve for *Hp*NikR was established based on a protocol as described previously [31,32]. *H. pylori* strain 26695 was cultured in BB medium supplemented with 0.2% β-cyclodextrin (Sigma) at 37 °C. At log phase (OD_{600} = 0.6), *H. pylori* cells were diluted to OD_{600} value of 0.35 and treated with or without 15 μg/mL of CBS and culture at 37 °C overnight. The *H. pylori* cells were then centrifuged on 5000*g* for 10 min at 4 °C. The medium was discarded and the cells were re-suspended in HEPES buffer (20 mM HEPES, 300 mM NaCl, pH 7.5). Equal amounts of cell suspensions from control and CBS-treated groups were aliquoted into PCR tubes and heated individually at different temperatures from 55 °C to 95 °C for 4 min followed by immediate cooling at 25 °C for 4 min. Each heating and cooling cycle was repeated three times. The cells were then lysed *via* 3 freeze-thaw cycles with liquid nitrogen. The cell lysates were centrifuged at 15,000*g* for 10 min at 4 °C to remove the precipitated protein. The supernatants were analyzed by gel electrophoresis and quantified by immuno-blotting using *Hp*NikR polyclonal antibodies.

2.8. RNA isolation and quantitative real time PCR

The *H. pylori* culture were cultured at 37 °C for 12 h in BB medium and grew until OD_{600} reached 0.6. The culture was then diluted to OD_{600} value of 0.3 and treated with 16 μg/mL CBS at 37 °C overnight. Total RNAs from both control and CBS-treated *H. pylori* were isolated with SV total RNA isolation kit (Promega) according to the manufacturer's instructions. cDNAs were generated by reverse transcription using GoScript Reverse Transcriptase (Promega). The transcription level of detected genes was determined by real-time PCR using GoTaq qPCR Master Mix kit (Promega) on a StepOnePlus Real-time PCR system (Life Technologies). The rrsA gene (16S rRNA) was used as an internal control. The primer pairs used to perform qPCR are listed in Table S1. The relative quantification of gene transcriptional levels was performed using the $2^{-\Delta\Delta Ct}$ method [33]. The mean value of control group was set as 1 and data were presented as mean ± sd and all experiments were conducted in triplicate.

3. Results and discussion

3.1. Bismuth binding property of HpNikR

Apo-form *Hp*NikR was expressed and purified as described in the experimental section [7]. To examine the bismuth binding property of *Hp*NikR, titration of apo-*Hp*NikR with Bi(III) was performed and monitored by UV–vis spectroscopy. In brief, aliquots of 2 mM CBS were added into 40 μM apo-*Hp*NikR in HEPES buffer (20 mM HEPES, 300 mM NaCl, 500 μM TCEP, pH 7.5). A broad absorption band centered at 360 nm was observed in the UV–vis spectra with the addition of Bi(III), which is assigned to π(S)(Cys) → Bi(III) ligand-to-metal charge transfer (Fig. 2a) [34]. Particularly, the absorption band reached maximum at a molar ratio of 1:1 ([Bi(III)]/[*Hp*NikR]), indicative of binding of one Bi(III) per *Hp*NikR monomer (Fig. 2a, inset). These results demonstrated that Bi(III) bound to apo-*Hp*NikR *via* cysteine residue.

In addition to Cys107 at the HA site, *Hp*NikR contains another cysteine residue (Cys96) at the tetramerization interface (Fig. 1) [8]. To further identify which cysteine was involved in Bi(III) binding, two cysteine residues were mutated to serine individually and titration of Bi (III) to the variants were monitored by UV–vis spectroscopy. No absorption bands were observed in UV–vis spectra when Bi(III) was titrated into *Hp*NikR^{C107S} variant, implying that Cys107 was likely involved in Bi(III) binding (Fig. S2a). In contrast, Bi(III) titration into *Hp*NikR^{C96S} variant led to a slow but visible increase of absorbance at 360 nm (Fig. S2b). It is implied that Bi(III) could bind to *Hp*NikR^{C96S} variant with a slow kinetics. Similar phenomenon was also observed for Ni(II) binding to *Hp*NikR^{C96S} [8]. Moreover, SEC and right angle light scattering showed that both wild-type (WT) *Hp*NikR and *Hp*NikR^{C107S} variant had a calculated molecular weight (MW) of 74.1 kDa, corresponding to a tetrameric *Hp*NikR (monomer: 17.1 kDa). In contrast, *Hp*NikR^{C96S} variant was eluted as a broad peak with a calculated molecular MW of 56.4 kDa, possibly implying an equilibrium between a dimeric and tetrameric form (Figs. S2c, S6a and b). Since the Cys96 is localized at the tetramerization interface, it is indicated that C96S mutagenesis caused *Hp*NikR tetramer dissociation, which could probably cause much slower binding of Bi(III) or Ni(II). On the other hand, Cys96 is relatively buried and inaccessible to Bi(III)-binding. The results demonstrate that only Cys107 at HA site was involved in Bi(III) binding. Indeed, no absorbance was observed at 360 nm when Bi(III) was titrated into Ni(II)-bound *Hp*NikR, in which case Cys107 was coordinated to Ni(II) (Fig. S2d).

To further investigate the Bi(III) binding capability of *Hp*NikR, 4 molar equivalents of Bi(III) (as bismuth nitrate) were incubated with 15 μM *Hp*NikR and excess amounts of metal ions were removed by HiTrap desalting column (GE healthcare). The bound Bi(III) contents were measured by ICP-MS and protein concentrations were determined by BCA assay as described previously [28]. Intriguingly, WT-*Hp*NikR could bind 2 molar equivalents of Bi(III) per monomer, implying that additional Bi(III) binding site existed besides the HA site (Fig. 2b). Indeed, the *Hp*NikR$^{C107S/H99A}$ variant, which does not contain the *Hp*NikR HA site could still bind 1 molar equivalent of Bi(III).

Previous studies demonstrated that *Hp*NikR contained two different Ni(II) coordination sites, including the 4-coordinated HA site and a 5/6 coordinated nickel site consisting of His74, His101, His88′ and water molecules [35]. To examine whether His74 and adjacent His75 residue participated in Bi(III) binding, *Hp*NikR$^{H74A/H75A}$ variant was prepared and identified to bind only 1 molar equivalent of Bi(III), indicating that the two residues are probably involved in Bi(III) binding (Fig. 2b). Furthermore, we investigated whether Bi(III) could replace Ni(II) at the two metal-sites. Consistent with previous report, NikR monomer could bind two molar equivalents of Ni(II) [36,37]. Subsequently, Ni(II)-bound NikR was incubated with different molar ratios of Bi(III) and the protein bound metal contents were measured by ICP-MS. The results indicated that only one Ni(II) site could be displaced by Bi(III) (Fig. S3A). In particular, the typical square planar Ni(II) *d-d* transition peak at 470 nm in UV–vis spectrum was not disturbed with increasing molar equivalents of Bi(III) (Fig. S3B) [38]. It is indicated that the Ni(II) at the HA site with square planar geometry could not be substituted by Bi(III).

3.2. Bi(III) binding induces HpNikR conformational change

Binding of non-physiological metal ions to proteins usually results in protein conformational changes [28,30,39]. Therefore, the effects of Bi(III) binding on the secondary structure of *Hp*NikR were first examined by CD spectroscopy (Fig. S4). The CD spectra were analyzed by the CAPITO Web server [40]. Deconvolution of the CD spectra of apo-*Hp*NikR gave rise to 66% α-helix and 10% β-sheet, while 52% α-helix and 13% β-sheet were found for Bi(III) bound *Hp*NikR, indicating that Bi(III)-binding perturbed *Hp*NikR secondary structure.

Previous studies demonstrated that Bi(III) binding usually led to aggregation of target protein, such as *H. pylori* Ni(II) chaperone HypB and DNA regulator Fur [28,30]. We subsequently investigated the oligomerization states of *Hp*NikR by SEC-MALS. In the absence of Bi(III),

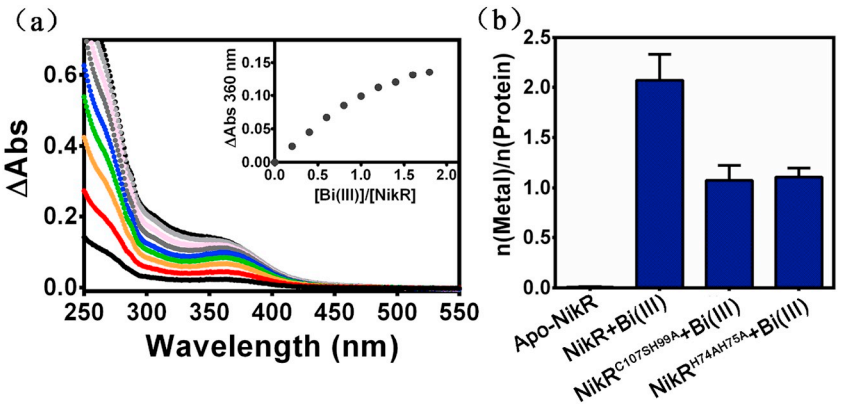

Fig. 2. Bi(III) binding of *Hp*NikR and variants monitored by UV–vis spectroscopy and ICP-MS. (a) UV–vis spectra of 40 μM apo-*Hp*NikR titrated by CBS. (b) ICP-MS analysis of Bi(III) binding capacities of *Hp*NikR and variants. The bound Bi(III) levels were determined by ICP-MS and proteins concentrations were measured by BCA assay.

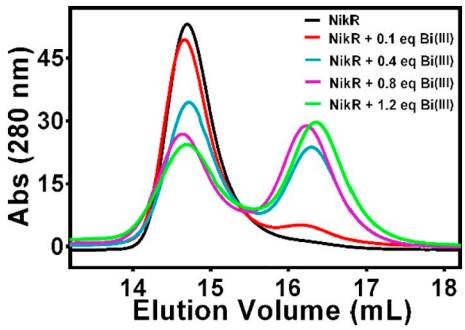

Fig. 3. Effects of Bi(III) binding on the oligomeric state of *Hp*NikR. Size-exclusion chromatography of apo-*Hp*NikR and *Hp*NikR incubated with 0.1, 0.4, 0.8 and 1.2 molar equivalences of Bi(III).

apo-*Hp*NikR was eluted as a tetramer with MW of 74.1 kDa, which is consistent with a previous report [41]. Unexpectedly, incubation of increasing amounts of Bi(III) with *Hp*NikR resulted in a new peak eluted at 16.2 mL on SEC column with an calculated MW of 33.8 kDa, implying the formation of dimeric *Hp*NikR upon Bi(III) binding (Fig. 3). The data indicated that Bi(III) binding completely changed *Hp*NikR quaternary structure, from a tetramer to a dimer.

Since *Hp*NikR contains two putative Bi(III) binding sites, we further examined which site was responsible for the Bi(III) induced disassembly of *Hp*NikR. The *Hp*NikR^{C107S} variant negated the HA site for Bi(III) binding, no evident disassembly was observed for *Hp*NikR^{C107S} variant in the presence of 4 molar equivalents of Bi(III) (Fig. S5a). In contrast, majority of *Hp*NikR$^{H74A/H75A}$ variant was eluted as the dimeric form upon incubation with Bi(III) (Fig. S5b), indicating that Bi(III) binding to the HA site led to the disassembly of *Hp*NikR. Given that the HA site was adjacent to two *Hp*NikR monomer interfaces, non-physiological Bi (III) binding could probably cause conformational distortion at the interfaces, which further resulted in *Hp*NikR tetramer disassembly.

3.3. Bi(III) abrogates HpNikR DNA-binding capability

*Hp*NikR is a pleiotropic DNA regulator and found to regulate directly or indirectly the expression of a series of genes involved in different functions [6]. For example, *Hp*NikR directly binds to the promoter region and activates the transcription of *ureAB* genes in the presence of Ni(II) [9,12,13]. Therefore, the effects of Bi(III) on DNA-binding capability of *Hp*NikR were investigated by EMSA. The *ureA* promoter DNA (P_{ureA}) is a well-established *Hp*NikR binding target [8,16]. Therefore, the P_{ureA} DNA fragment was amplified by PCR using primers listed in Table S1. 80 nM P_{ureA} DNA probe was incubated with gradient amounts of *Hp*NikR in the presence of 800 μM Ni(II). As shown in Fig. 4a, a significant shift of the P_{ureA} probe was observed in the EMSA, indicating the formation of *Hp*NikR-DNA complex in the

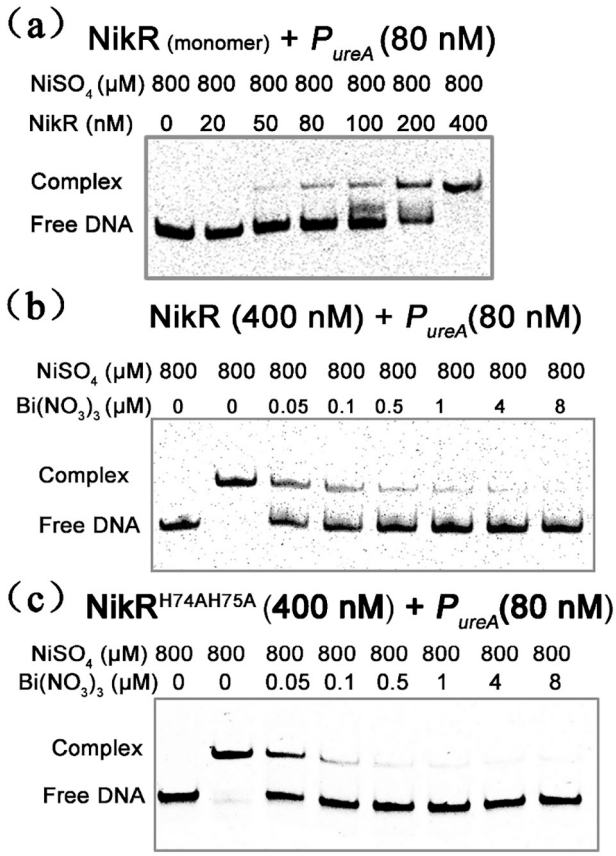

Fig. 4. Electrophoretic mobility shift assay (EMSA) of WT-*Hp*NikR and *Hp*NikR$^{H74A/H75A}$ variant binding to the *ureA* promoter DNA (P_{ureA}). (a) 80 nM P_{ureA} DNA were incubated with gradient amounts of *Hp*NikR in the presence of 800 μM Ni(II). 400 nM WT-*Hp*NikR (monomer) (b) and *Hp*NikR$^{H74A/H75A}$ variant (c) were incubated with increasing concentration of Bi(III) in the presence of 80 nM P_{ureA} DNA and 800 μM Ni(II).

presence of Ni(II). In contrast, *Hp*NikR did not bind to a negative control *rpoB* promoter (P_{rpoB}) under similar condition (Fig. S7). Whereas, supplementation of gradient amounts of Bi(III) to the mixture of 400 nM *Hp*NikR (monomer), P_{ureA} probe significantly ruptured the *Hp*NikR-DNA complex, resulting dissociation of P_{ureA} DNA from *Hp*NikR. Typically, 20 molar equivalences of Bi(III) could completely negate the *Hp*NikR-DNA complex, indicating that Bi(III) binding attenuated the DNA binding capability of *Hp*NikR (Fig. 4b).

Similar to the WT-*Hp*NikR, the *Hp*NikR$^{H74A/H75A}$ variant, which retains the HA Ni(II) site, could still bind to the P_{ureA} DNA. However, the variant protein is even more vulnerable to Bi(III) binding as no *Hp*NikR-DNA complex was visible in the presence of 10 molar

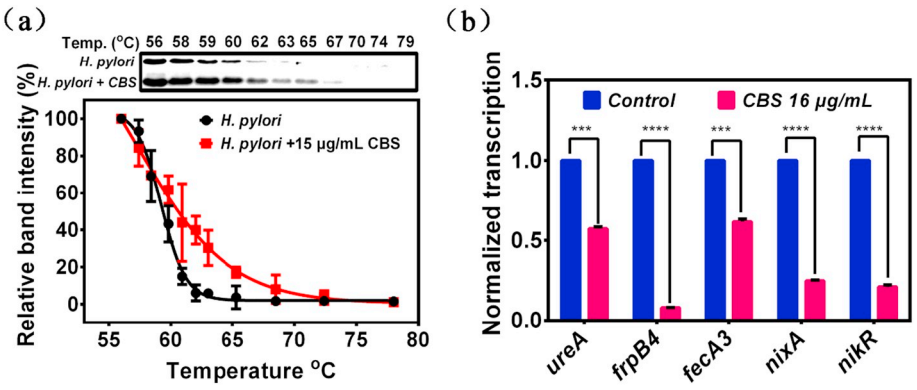

Fig. 5. (a) Cellular thermal shift assay of *H. pylori* bacteria with or without 15 μg/mL of CBS treatment. The band intensities at different temperatures are normalized to that at 56 °C. All experiments were performed in triplicates. (b) Quantitative transcription analysis of *ureA*, *frpB4*, *fecA3*, *nixA* and *nikR* genes with or without 16 μg/mL of CBS treatment. The mean values of the transcription level of untreated groups are set as 1. Results are shown as mean ± sd. The statistical difference is determined by two-tailed Student's *t*-test.

equivalences of Bi(III) (Fig. 4c). The data further verified that Bi(III) binding to the HA Ni(II) site ablated the DNA binding capability of *Hp*NikR.

3.4. HpNikR is an intracellular target of Bi(III)

We have demonstrated that Bi(III) bound to *Hp*NikR and negated its regulatory functionality *in vitro*. To further examine whether *Hp*NikR is an intracellular target of Bi(III), the CETSA was employed to investigate the interaction between *Hp*NikR and Bi(III) *in vivo* as previously described [32,42]. In brief, sub-lethal doses of CBS with a final concentration of 15 μg/mL were added into *H. pylori* culture. The thermal denaturation curves of *Hp*NikR with and without (negative control groups) addition of CBS were plotted. As shown in Fig. 5a, the aggregation temperature (T_{agg}) of intracellular *Hp*NikR was shifted from 59 °C to 61 °C after CBS treatment, indicating that Bi(III) bound to *Hp*NikR in bacterial cell. Furthermore, the results are also consistent with protein denaturation assay of purified *Hp*NikR *in vitro*, which further demonstrated that Bi(III) binding could enhance *Hp*NikR thermal stability (Fig. S8).

As a global regulator, *Hp*NikR is involved in the transcription of multiple genes. However, only a few of the genes have been identified as direct *Hp*NikR targets. For example, *Hp*NikR activates the transcription of *ureAB* and represses *nikR*, *exbB-exbD-tonB*, *nixA*, *frpB4*, *fecA3* and *fur* genes in the presence of Ni(II) [6,9,43]. To investigate the effects of Bi(III) on the regulatory function of *Hp*NikR *in vivo*, we examined the transcriptional levels of five different *Hp*NikR regulated genes, including *ureA*, *frpB4*, *fecA3*, *nixA* and *nikR*. The gene *ureA* encodes the α-subunit of *H. pylori* urease [44]. FrpB4 and FecA3 are outer membrane proteins involved in iron uptake [45,46]. And NixA is also a high-affinity nickel permease of *H. pylori* [47]. As shown in Fig. 5b, the mRNA transcriptional levels of all these five genes are significantly attenuated after treatment of *H. pylori* with 16 μg/mL CBS, indicating that Bi(III) treatment remarkably perturbed the transcription of *Hp*NikR-regulated genes. It should be noted that *frpB4*, *fecA3*, *nixA* and *nikR* genes are repressed by Ni(II)-bound *Hp*NikR. Therefore, functionality abrogation of *Hp*NikR by Bi(III) should enhance the transcriptional levels of these genes. This discrepancy could be probably due to the multi-targeted properties of Bi(III), which might interfere with the transcription of the genes by other means. For example, it is reported that the transcription of *frpB4* and *fecA3* genes are also under the control of ferric uptake regulator (Fur), which has also been identified as an intracellular target of bismuth drug [30].

4. Conclusion and perspective

In conclusion, we demonstrate that a clinically used bismuth-based drug CBS targets NikR from *H. pylori via* the highly conserved residue Cys107 to the HA site of apo-form *Hp*NikR. Importantly, Bi(III)-binding disassembles apo-*Hp*NikR from a functional tetramer into an inactive dimer, which negates its DNA binding capability both *in vitro* and *in vivo*. NikR and Fur are two major DNA regulators in *H. pylori*. The homeostasis of two essential metal nutrients, *i.e.*, iron and nickel, are orchestrated by the two regulators. They are also critical for *H. pylori* to thrive in the inhospitable environment of human stomach [48]. The bismuth-based drugs could significantly perturb the physiological metal metabolism of *H. pylori via* targeting the two essential regulator proteins, which contributes to its anti-bacterial activities.

Abbreviations

DBD	DNA-binding domain
MBD	metal-binding domain
HA site	high-affinity nickel binding site
BSS	bismuth subsalicylate
CBS	colloidal bismuth subcitrate
E. coli	*Escherichia coli*
LB	Luria-Bertani
BB	Brucella Broth
IPTG	isopropyl-β-D-thiogalactopyranoside
PMSF	phenylmethylsulfonyl fluoride
EDTA	ethylenediaminetetraacetic acid
TCEP	Tri(2-chloroethyl) phosphate
ICP-MS	inductively coupled plasma mass spectrometry
BCA	bicinchoninic acid
CD	circular dichroism
SEC	size-exclusion chromatography
EMSA	electrophoretic mobility shift assays
PCR	polymerase chain reaction
CETSA	cellular thermal shift assay
qPCR	quantitative real time PCR
MW	molecular weight
HEPES	2 hydroxyethylpiperazine-N-2 ethane sulfonic acid
DTT	dithiothreitol

Acknowledgements

This work was supported by the National Natural Science Foundation of China (21671203, 21877131), Guangzhou Science and Technology Program key projects (201707010038), RGC, UGC of Hong Kong (17305415, 17333616), the Ministry of Education of China (IRT-17R111), the Fundamental Research Funds for the Central Universities and a start funding from Sun Yat-sen University.

Appendix A. Supplementary data

Supplementary data to this article can be found online at https://doi.org/10.1016/j.jinorgbio.2019.03.025.

References

[1] J.G. Kusters, A.H. van Vliet, E.J. Kuipers, Clin. Microbiol. Rev. 19 (2006) 449–490.
[2] H. Nakamura, H. Yoshiyama, H. Takeuchi, T. Mizote, K. Okita, T. Nakazawa, Infect. Immun. 66 (1998) 4832–4837.
[3] A.H. van Vliet, F.D. Ernst, J.G. Kusters, Trends Microbiol. 12 (2004) 489–494.
[4] J.W. Olson, R.J. Maier, Science 298 (2002) 1788–1790.
[5] S. Bury-Mone, J.M. Thiberge, M. Contreras, A. Maitournam, A. Labigne, H. De Reuse, Mol. Microbiol. 53 (2004) 623–638.
[6] M. Contreras, J.M. Thiberge, M.A. Mandrand-Berthelot, A. Labigne, Mol. Microbiol. 49 (2003) 947–963.
[7] C. Dian, K. Schauer, U. Kapp, S.M. McSweeney, A. Labigne, L. Terradot, J. Mol. Biol. 361 (2006) 715–730.
[8] C. Bahlawane, C. Dian, C. Muller, A. Round, C. Fauquant, K. Schauer, H. de Reuse, L. Terradot, I. Michaud-Soret, Nucleic Acids Res. 38 (2010) 3106–3118.
[9] F.D. Ernst, E.J. Kuipers, A. Heijens, R. Sarwari, J. Stoof, C.W. Penn, J.G. Kusters, A.H. van Vliet, Infect. Immun. 73 (2005) 7252–7258.
[10] A.L. West, F. St John, P.E. Lopes, A.D. MacKerell Jr., E. Pozharski, S.L. Michel, J. Am. Chem. Soc. 132 (2010) 14447–14456.
[11] S. Benini, M. Cianci, S. Ciurli, Dalton Trans. 40 (2011) 7831–7833.
[12] L.O. Abraham, Y. Li, D.B. Zamble, J. Inorg. Biochem. 100 (2006) 1005–1014.
[13] N.S. Dosanjh, N.A. Hammerbacher, S.L. Michel, Biochemistry 46 (2007) 2520–2529.
[14] N.S. Dosanjh, S.L.J. Michel, Curr. Opin. Chem. Biol. 10 (2006) 123–130.
[15] B. Zambelli, M. Bellucci, A. Danielli, V. Scarlato, S. Ciurli, Chem. Commun. (2007) 3649–3651.
[16] B. Zambelli, A. Danielli, S. Romagnoli, P. Neyroz, S. Ciurli, V. Scarlato, J. Mol. Biol. 383 (2008) 1129–1143.
[17] F. Musiani, B. Bertosa, A. Magistrato, B. Zambelli, P. Turano, V. Losasso, C. Micheletti, S. Ciurli, P. Carloni, J. Chem. Theory Comput. 6 (2010) 3503–3515.
[18] E. Fabini, B. Zambelli, L. Mazzei, S. Ciurli, C. Bertucci, Anal. Bioanal. Chem. 408 (2016) 7971–7980.
[19] E.R. Schreiter, S.C. Wang, D.B. Zamble, C.L. Drennan, Proc. Natl. Acad. Sci. U. S. A. 103 (2006) 13676–13681.
[20] L. Mazzei, O. Dobrovolska, F. Musiani, B. Zambelli, S. Ciurli, J. Biol. Inorg. Chem. 20 (2015) 1021–1037.
[21] A.J. Wagstaff, P. Benfield, J.P. Monk, Drugs 36 (1988) 132–157.
[22] W. Li, L. Jin, N. Zhu, X. Hou, F. Deng, H. Sun, J. Am. Chem. Soc. 125 (2003) 12408–12409.
[23] G. Treiber, P. Malfertheiner, U. Klotz, Expert. Opin. Pharmacother. 8 (2007) 329–350.
[24] M.P. Dore, H. Lu, D.Y. Graham, Gut 65 (2016) 870–878.
[25] S. Marchi, F. Costa, M. Bellini, C. Belcari, M.G. Mumolo, A. Tornar, R. Spisni, E. Torelli, G. Maltinti, Eur. J. Gastroenterol. Hepatol. 13 (2001) 547–550.
[26] Y. Wang, L. Hu, F. Xu, Q. Quan, Y.T. Lai, W. Xia, Y. Yang, Y.Y. Chang, X. Yang, Z. Chai, J. Wang, I.K. Chu, H. Li, H. Sun, Chem. Sci. 8 (2017) 4626–4633.
[27] Y. Wang, C.N. Tsang, F. Xu, P.W. Kong, L. Hu, J. Wang, I.K. Chu, H. Li, H. Sun, Chem. Commun. 51 (2015) 16479–16482.
[28] W. Xia, H. Li, H. Sun, Chem. Commun. 50 (2014) 1611–1614.
[29] Y.Y. Chang, T. Cheng, X. Yang, L. Jin, H. Sun, H. Li, J. Biol. Inorg. Chem. 22 (2017) 673–683.
[30] X. He, X. Liao, H. Li, W. Xia, H. Sun, Inorg. Chem. 56 (2017) 15041–15048.
[31] R. Jafari, H. Almqvist, H. Axelsson, M. Ignatushchenko, T. Lundback, P. Nordlund, D. Martinez Molina, Nat. Protoc. 9 (2014) 2100–2122.
[32] D. Martinez Molina, R. Jafari, M. Ignatushchenko, T. Seki, E.A. Larsson, C. Dan, L. Sreekumar, Y. Cao, P. Nordlund, Science 341 (2013) 84–87.
[33] K.J. Livak, T.D. Schmittgen, Methods 25 (2001) 402–408.
[34] H. Sun, H. Li, I. Harvey, P.J. Sadler, J. Biol. Chem. 274 (1999) 29094–29101.
[35] A.L. West, S.E. Evans, J.M. Gonzalez, L.G. Carter, H. Tsuruta, E. Pozharski, S.L. Michel, Proc. Natl. Acad. Sci. U. S. A. 109 (2012) 5633–5638.
[36] B. Zambelli, M. Bellucci, A. Danielli, V. Scarlato, S. Ciurli, Chem. Commun. (2007) 3649–3651.
[37] S. Leitch, M.J. Bradley, J.L. Rowe, P.T. Chivers, M.J. Maroney, J. Am. Chem. Soc. 129 (2007) 5085–5095.
[38] C. Fauquant, R.E.M. Diederix, A. Rodrigue, C. Dian, U. Kapp, L. Terradot, M.A. Mandrand-Berthelot, I. Michaud-Soret, Biochimie 88 (2006) 1693–1705.
[39] S. Cun, H. Sun, Proc. Natl. Acad. Sci. U. S. A. 107 (2010) 4943–4948.
[40] C. Wiedemann, P. Bellstedt, M. Gorlach, Bioinformatics 29 (2013) 1750–1757.
[41] E.L. Benanti, P.T. Chivers, J. Biol. Chem. 286 (2011) 15728–15737.
[42] D.M. Molina, P. Nordlund, Annu. Rev. Pharmacol. Toxicol. 56 (2016) 141–161.
[43] I. Delany, R. Ieva, A. Soragni, M. Hilleringmann, R. Rappuoli, V. Scarlato, J. Bacteriol. 187 (2005) 7703–7715.
[44] N.C. Ha, S.T. Oh, J.Y. Sung, K.A. Cha, M.H. Lee, B.H. Oh, Nat. Struct. Biol. 8 (2001) 505–509.
[45] I. Delany, A.B. Pacheco, G. Spohn, R. Rappuoli, V. Scarlato, J. Bacteriol. 183 (2001) 4932–4937.
[46] O.Q. Pich, D.S. Merrell, Future Microbiol 8 (2013) 725–738.
[47] H.L. Mobley, R.M. Garner, P. Bauerfeind, Mol. Microbiol. 16 (1995) 97–109.
[48] K.P. Haley, J.A. Gaddy, Front. Microbiol. 6 (2015) 911–912.